

Superresolution underwater acoustics

Annie Cuyt, Wen-shin Lee, Engelbert Tijskens
Department of Mathematics and Computer Science, Universiteit Antwerpen, Belgium

Wen-Ling Hong, Jr-Ping Wang
Department of Naval Architecture and Ocean Engineering, National Kaohsiung University of Science and Technology, Taiwan

Tim Cools, Tim Geerts
Antwerp Maritime Academy, Belgium

Summary

We explore the application of some recent results in exponential analysis and sparse interpolation to underwater acoustics, in a joint effort from marine engineers and computational mathematicians. The fact that, in practice, the sampling rate used for the recording of an echoed signal is often a multiple of the Nyquist rate, is regarded as a constraint on the cost and performance of echo sounding devices.

Here we illustrate how the latter can be overcome, using a new regular sampling scheme, that can even go well below the Nyquist rate. In the numerical examples an average of 20-25 % of the Nyquist rate is amply sufficient to reliably recognize and reconstruct the echo. The sparse sub-Nyquist method under consideration allows to recover from possible aliasing introduced by the subsampling.

The technique does not need newly designed hardware, has low computational complexity and uses a small number of samples.

PACS no. 43.25.Jh, 43.30.Gv, 43.60.Jn

1. Introduction

The applications of underwater sound analysis span a wide range, including positioning, navigation, wireless communication, echo-sounding, seabed mapping, geophysical surveying, water quality measurement, active and passive sonar, military intelligence, and oceanic measurements such as wave heights, ocean currents and temperature. Underwater acoustics is also a key underpinning technology in offshore oil and gas activities, is increasingly used in oceanographic and environmental studies, and continues to play a crucial role in defence. Its fundamental role cannot be overstated.

In signal processing data are traditionally sampled uniformly at a rate dictated by the Shannon-Nyquist theorem, which states that the sampling rate needs to be at least twice the maximum bandwidth of the signal. A coarser time grid than dictated by the theory of Nyquist and Shannon causes aliasing, mapping higher frequencies to lower ones in the analysis. Here we introduce a procedure for underwater acoustics that works with sub-sampled data: our parametric

method samples at a rate below the Shannon-Nyquist one while maintaining a regular sampling scheme.

The key idea is quite generic so that it can be combined [2, 1] with several popular signal processing procedures, both parametric and non-parametric, such as ESPRIT [14], MUSIC [15], the matrix pencil [10] algorithm, variable projection methods [13], and the discrete Fourier transform. We illustrate some of these possibilities on real-life hydrophone recordings.

2. Classical exponential analysis

Consider the interpolation problem

$$f_j = \sum_{i=1}^n \alpha_i \exp(\phi_i t_j), \quad \alpha_i, \phi_i \in \mathbb{C} \quad (1)$$

from the values f_j at the uniformly spaced interpolation points t_j . We assume that the frequency content in (1) is limited by [12, 16]

$$|\Im(\phi_i)|/(2\pi) = |\omega_i| < \Omega/2, \quad i = 1, \dots, n, \quad (2)$$

and that the $2n$ sample points $t_j = j\Delta$ are spaced with $\Delta \leq 1/\Omega$. In the sequel we also assume that n is known, as its computation is less relevant in the current application. Techniques for the extraction of

the value of n from the samples f_j can be found in [4, 11, 2]. The interpolation problem (1) consists in estimating the parameters ϕ_1, \dots, ϕ_n and $\alpha_1, \dots, \alpha_n$ from the samples f_j at the points t_j .

Let us define the Hankel matrix

$${}^{\rho}_1 H_n := \begin{bmatrix} f_{\rho} & \cdots & f_{\rho+n-1} \\ \vdots & \ddots & \vdots \\ f_{\rho+n-1} & \cdots & f_{\rho+2n-2} \end{bmatrix}, \quad \rho \in \mathbb{Z}.$$

It is well-known that the Hankel matrix ${}^{\rho}_1 H_n$ can be decomposed as

$${}^{\rho}_1 H_n = V_n \Lambda_n A_n V_n^T,$$

$$V_n = \begin{bmatrix} 1 & \cdots & 1 \\ \exp(\phi_1 \Delta) & \cdots & \exp(\phi_n \Delta) \\ \vdots & & \vdots \\ \exp(\phi_1(n-1)\Delta) & \cdots & \exp(\phi_n(n-1)\Delta) \end{bmatrix},$$

$$A_n = \text{diag}(\alpha_1, \dots, \alpha_n),$$

$$\Lambda_n = \text{diag}(\exp(\phi_1 \rho \Delta), \dots, \exp(\phi_n \rho \Delta)).$$

For chosen ρ , the values $\exp(\phi_i \Delta)$ can be retrieved from the generalized eigenvalue problem [10]

$$\begin{pmatrix} \rho+1 \\ 1 \end{pmatrix} H_n v_i = \exp(\phi_i \Delta) \begin{pmatrix} \rho \\ 1 \end{pmatrix} H_n v_i, \quad i = 1, \dots, n, \quad (3)$$

where v_i are the generalized right eigenvectors. The choice $\rho = 0$ coincides with the original solution of the interpolation problem already proposed in 1795 by de Prony [8]. From the $\exp(\phi_i \Delta)$, the complex numbers ϕ_i are uniquely defined because of the restriction $|\Im(\phi_i \Delta)| < \pi$. Subsequently the remaining linear coefficients $\alpha_i, i = 1, \dots, n$ are obtained from the linear system of interpolation conditions

$$\sum_{i=1}^n \alpha_i \exp(\phi_i j \Delta) = f_j, \quad j = 0, \dots, 2n-1 \quad (4)$$

which can be solved in the least squares sense in the case of noisy data or exactly in the case of exact data (in the latter case n of the interpolation conditions are linearly dependent because the ϕ_i satisfy the generalized eigenvalue problem). We remark that the coefficient matrix of (4) is a Vandermonde matrix.

In the noisy case the structured matrices in both (3) and (4) can also be extended to rectangular $N \times n$ matrices with $N > n$ and (3) and (4) can be considered in the least squares sense [13]. Then the index j in (4) runs from 0 to $N + n - 1$ and the total sample usage equals $N + n$.

3. Sub-Nyquist exponential analysis

Now let us consider more general sample locations $t_{\rho+jr} = (\rho+jr)\Delta$ with $r \in \mathbb{N}, r > 1$ and $\text{gcd}(r, \rho) = 1$.

For chosen ρ and r we denote the sample at $t_{\rho+jr}, j = 0, \dots, 2n-1$ by $f_{\rho+jr}$. The interpolation problem now becomes

$$f_{\rho+jr} = \sum_{i=1}^n \alpha_i \exp(\phi_i(\rho+jr)\Delta),$$

where j runs for $\rho = 0$ (at least) from 0 to $2n-1$ and for some $\rho \neq 0$ (at least) from 0 to $n-1$. With $r \in \mathbb{N}, \rho \in \mathbb{Z}$ we now define

$${}^{\rho}_r H_n := \begin{bmatrix} f_{\rho} & f_{\rho+r} & \cdots & f_{\rho+(n-1)r} \\ f_{\rho+r} & & & \vdots \\ \vdots & \ddots & & \vdots \\ f_{\rho+(n-1)r} & \cdots & & f_{\rho+(2n-2)r} \end{bmatrix}.$$

This Hankel matrix ${}^{\rho}_r H_n$ is decomposable as

$${}^{\rho}_r H_n = V_n \Lambda_n A_n V_n^T,$$

$$V_n = \begin{bmatrix} 1 & \cdots & 1 \\ \exp(\phi_1 r \Delta) & \cdots & \exp(\phi_n r \Delta) \\ \vdots & & \vdots \\ \exp(\phi_1(n-1)r\Delta) & \cdots & \exp(\phi_n(n-1)r\Delta) \end{bmatrix},$$

$$A_n = \text{diag}(\alpha_1, \dots, \alpha_n),$$

$$\Lambda_n = \text{diag}(\exp(\phi_1 \rho \Delta), \dots, \exp(\phi_n \rho \Delta)).$$

Again the values $\exp(\phi_i r \Delta)$, now with $r > 1$, can be obtained from the generalized eigenvalue problem

$$\begin{pmatrix} \rho+r \\ r \end{pmatrix} H_n v_i = \exp(\phi_i r \Delta) \begin{pmatrix} \rho \\ r \end{pmatrix} H_n v_i, \quad i = 1, \dots, n, \quad (5)$$

where v_i are the generalized right eigenvectors. With $r > 1$ the ϕ_i cannot be retrieved uniquely from the generalized eigenvalues $\exp(\phi_i r \Delta)$ anymore because

$$|\Im(\phi_i r \Delta)| < r\pi. \quad (6)$$

Choosing $r > 1$ offers several numerical advantages though [9, 7, 3] besides the fact that one can work with sub-Nyquist sampled data [5, 6]. Especially when Ω is quite large, the latter may be interesting as $\Delta \leq 1/\Omega$ may become so small that collecting the samples f_j becomes costly.

We now indicate how to resolve (6). First of all, with $\rho = 0$, the linear coefficients $\alpha_i, i = 1, \dots, n$ are computed from the linear system

$$\sum_{i=1}^n \alpha_i \exp(\phi_i j r \Delta) = f_{jr}, \quad j = 0, \dots, 2n-1.$$

Next, for chosen ρ , a shifted set of at least n samples $f_{\rho+jr}$ is interpreted as

$$f_{\rho+jr} = \sum_{i=1}^n (\alpha_i \exp(\phi_i \rho \Delta)) \exp(\phi_i j r \Delta), \quad \rho \in \mathbb{Z}. \quad (7)$$

Note that (7) is merely a shifted version of the original problem where the effect of the shift is pushed into the coefficient. From (7) the coefficients $\alpha_i \exp(\phi_i \rho \Delta)$ can be computed since the generalized eigenvalues $\exp(\phi_i r \Delta)$ are known. From the α_i and the $\alpha_i \exp(\phi_i \rho \Delta)$ we obtain

$$\frac{\alpha_i \exp(\phi_i \rho \Delta)}{\alpha_i} = \exp(\phi_i \rho \Delta),$$

from which again the ϕ_i cannot be extracted unambiguously if $\rho > 1$. But if $\gcd(r, \rho) = 1$ the sets

$$\left\{ \exp\left(\phi_i \Delta + \frac{2\pi i}{r} \ell\right), \ell = 0, \dots, r-1 \right\}$$

and

$$\left\{ \exp\left(\phi_i \Delta + \frac{2\pi i}{\rho} \ell\right), \ell = 0, \dots, \rho-1 \right\},$$

which contain all the possible values for $\exp(\phi_i \Delta)$ obtained respectively from $\exp(\phi_i r \Delta)$ in (3) and $\exp(\phi_i \rho \Delta)$ in (7), have a unique intersection [7]. How to obtain this and identify the ϕ_i is detailed in [7, 3]. So at this point the nonlinear parameters $\phi_i, i = 1, \dots, n$ and the linear $\alpha_i, i = 1, \dots, n$ in (1) are computed through the solution of either (3) or (5) and (4), and if $r > 1$ also (7). Remedying the aliasing introduced by taking $r > 1$ is consequently at the expense of another n samples at shifted locations $t_{\rho+jr}$.

As in the previous section, the structured matrices in the generalized eigenvalue problem (5) can be extended to $N \times n$ matrices with $N > n$. Likewise, the structured linear system (7) expressing the shifted samples, can be extended and solved in the least squares sense. For the latter we can for instance consider the size $\lfloor (N+n)/2 \rfloor \times n$.

4. Application to echosounder signals

The sub-Nyquist analysis can easily be combined with existing implementations such as ESPRIT, MUSIC, the matrix pencil algorithm or variable projection, as indicated in [2]. It can also be incorporated in a classical Fourier analysis which then turns this into a sparse Fourier method, as developed in [1]. For our numerical illustrations we use the basic underlying method outlined in [7] which is summarized in the previous sections.

We consider two hydrophone recordings, respectively made:

1. at the test pool of the National Kaohsiung University of Science and Technology in Taiwan,
2. and in open water by the Antwerp Maritime Academy associated with the University of Antwerp in Belgium.

4.1. Test pool recording

The test pool is 1 m deep with a surface of 1.8 m by 1.8 m and for the experiment a Lowrance fishfinder was used. The recording was of an 83 kHz outgoing signal, about 30-fold oversampled at 5 MHz (the Nyquist rate being 166 kHz), and of an incoming echo with the same frequency, about 75-fold oversampled at 12.5 MHz. Extracts of both are displayed in Figure 1.

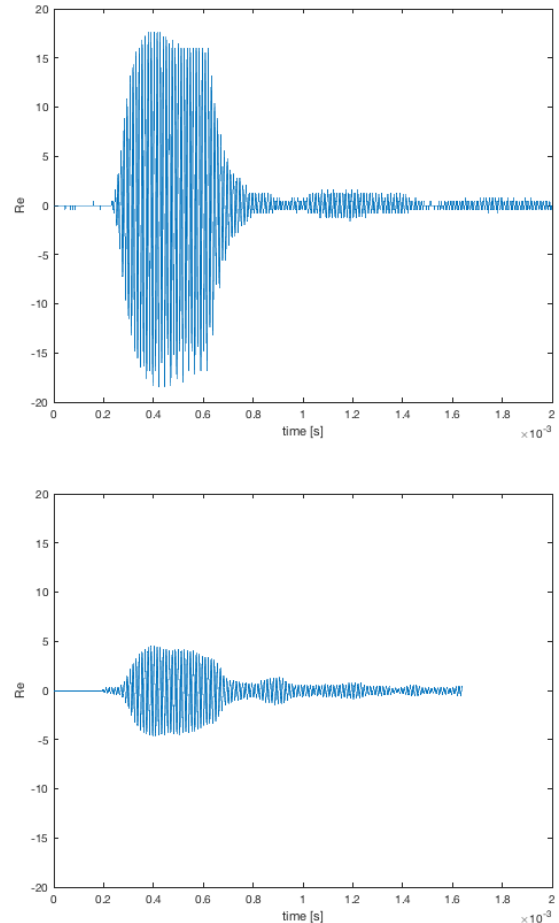


Figure 1. Extracted pulse from the sent (top) and received (bottom) signal.

Since we only process the middle part of the recorded pulses, we can take $n = 4$ so that 2 exponential terms model the sinusoidal signal and an additional 2 terms absorb the noise in each pulse. In Figure 2 at the left we show the middle 1500 samples of a sent pulse and at the right the 2400 retained samples of a received pulse. With $r = 194, \rho = 11$ for the sent signal and $r = 317, \rho = 13$ for the received signal, the frequency of 83 kHz is reliably extracted from the minimal number of $3n = 12$ samples taken at the points $t_{jr}, j = 0, \dots, 7$ and $t_{\rho+jr}, j = 0, \dots, 3$. For the sent signal the estimate of 82.8 kHz is returned

and for the received one 82.4 kHz. This undersampling and shifting strategy is comparable to the use of recordings at 23% and 35% of the Nyquist rate for the sent and received signal respectively.

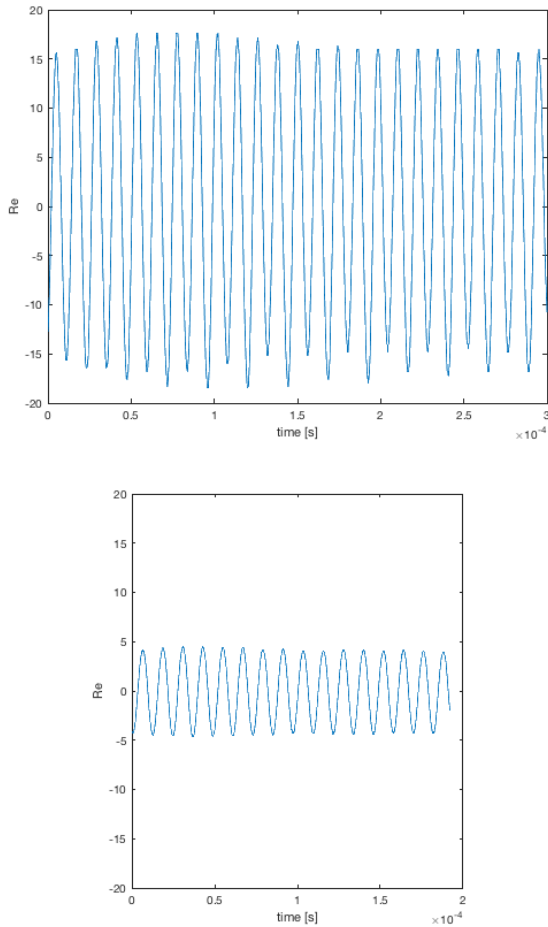


Figure 2. Analyzed extract from the sent (top) and received (bottom) signal.

When adding more samples, the square Hankel and Vandermonde matrices are extended to overdetermined rectangular ones and the problems can be dealt with in the least squares sense. But in the test pool setup the noise is not so large that this is necessary.

In Figure 3 the reconstruction based on (1) (shown in red) of the signal shown in Figure 2 is plotted on top of the original (shown in blue). It is clear that the exponential model extracted from only 12 samples collected at a rate well below the Nyquist rate is quite accurate.

4.2. Open water recording

The recording in open water was performed using a Humminbird fishfinder at a sampling rate of 2 MHz. The instrument’s emitted downward beam is 200 kHz and the two side beams are 455 kHz. We analyze

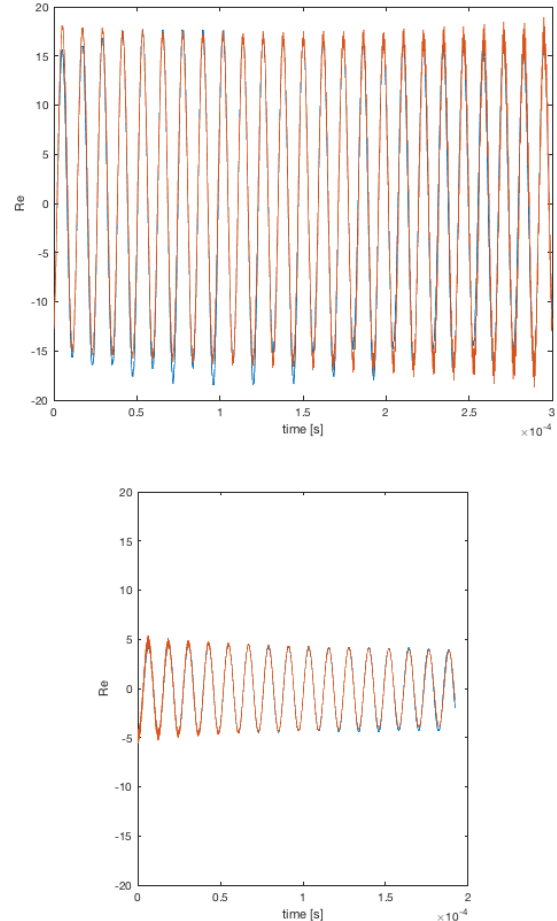


Figure 3. Reconstructed extract from the sent (top) and received (bottom) signal.

and reconstruct the echos on the side beams that are shown in Figure 4. In a first step, we restrict the analysis to some middle part of the echos, namely some 190 samples for the first echo and some 130 samples for the second one, as shown in Figure 5.

We take $r = 7, \rho = 3$ and $n = 8$, giving us six terms to model the somewhat larger noise in addition to the standard two terms representing the instrument’s outgoing frequency. Instead of the minimal of $3n = 24$ samples, we enlarge all structured matrices with additional rows making the generalized eigenvalue problem and the Vandermonde system overdetermined.

For the first echo we solve an $N \times n = 20 \times 8$ generalized eigenvalue problem requiring 28 samples at the points $t_{jr}, j = 0, \dots, 27$ and we solve an $\lfloor (N + n)/2 \rfloor \times n = 14 \times 8$ Vandermonde system requiring 14 samples at the shifted time points $t_{\rho+jr}, j = 0, \dots, 13$. The frequency of 455 kHz is recovered with a relative error of only 1.7%, namely at 462.8 kHz.

For the second echo we solve an 11×8 generalized eigenvalue problem from 19 samples and a 9×8 Vandermonde system needing 9 samples, resulting in an estimate of 461.4 kHz for the frequency or a relative error of only 1.4%.

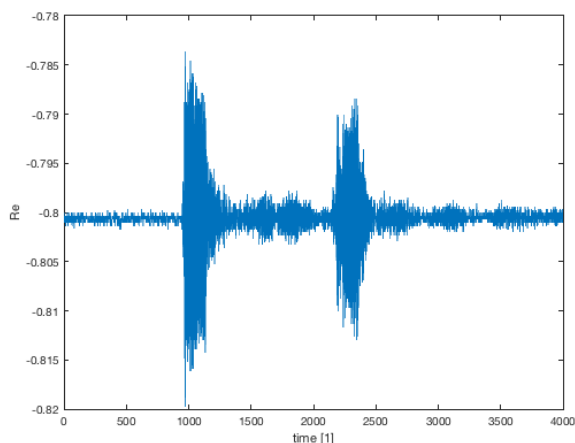


Figure 4. Two echoed pulses recorded in the open water experiment.

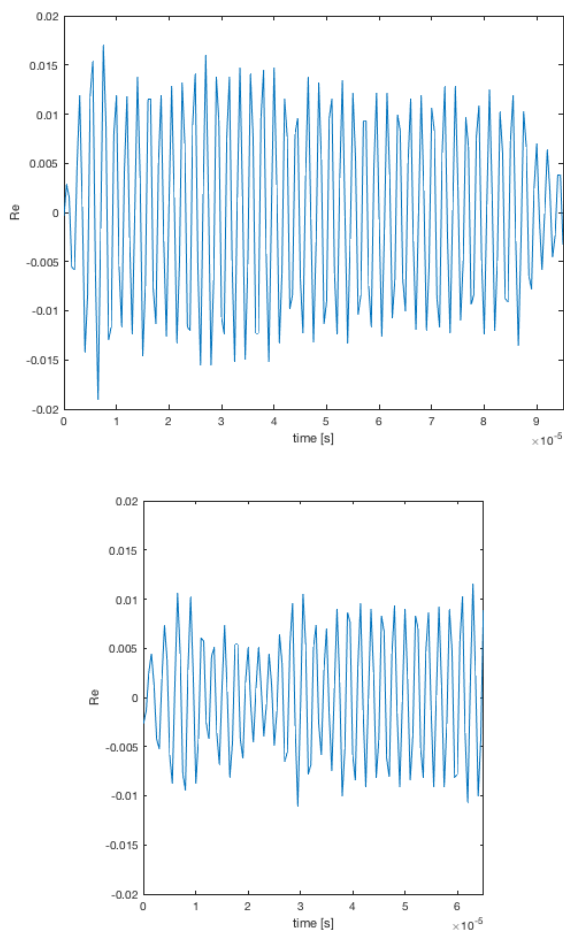


Figure 5. Analyzed extract from the first (top) and second (bottom) echoed pulse.

Both analyses, considering the undersampling and the shifting jointly, are comparable to using a sampling scheme at only 21% of the Nyquist rate. The undersampling solely is comparable to a sampling scheme at somewhat more than 14% of the Nyquist

rate. The shifted samples added uniformly inbetween account for almost an additional 7%. We also remark that the output delivered by our scheme is more accurate than a full ESPRIT analysis of all respectively 191 and 131 samples, when solving for $n = 8$ terms.

Acknowledgement

The UA Antwerpen and Antwerp Maritime Academy authors were partially supported by the “BOF-academiseren” grant entitled “Sub-Nyquist underwater communication”.

The authors from the National Kaohsiung University of Science and Technology thank Chien-Erh Weng and Ruey-Chang Wei for kindly providing the Lowrance fishfinder and hydrophone used in the experiments.

References

- [1] M. Briani, A. Cuyt, and W.-s. Lee. A hybrid Fourier-Prony method. ArXiv e-print 1706.04520 [math.NA], Universiteit Antwerpen, 2017.
- [2] M. Briani, A. Cuyt, and W.-s. Lee. Validated exponential analysis for harmonic sounds. In *DAFX17, 20th international conference on digital audio effects*, volume 20, pages 222–227, Edinburgh, United Kingdom, 2017.
- [3] M. Briani, A. Cuyt, and W.-s. Lee. VEXPA: Validated EXPonential Analysis through regular subsampling. ArXiv e-print 1709.04281 [math.NA], Universiteit Antwerpen, 2017.
- [4] A. Cuyt, M.-n. Tsai, M. Verhoye, and W.-s. Lee. Faint and clustered components in exponential analysis. *Applied Mathematics and Computation*, 327:93–103, 2018.
- [5] A. Cuyt and W.-s. Lee. Smart data sampling and data reconstruction. Patent PCT/EP2012/066204.
- [6] A. Cuyt and W.-s. Lee. Smart data sampling and data reconstruction. US Patent 9,690,749.
- [7] A. Cuyt and W.-s. Lee. How to get high resolution results from sparse and coarsely sampled data. ArXiv e-print 1710.09694 [math.NA], Universiteit Antwerpen, 2017.
- [8] R. de Prony. Essai expérimental et analytique sur les lois de la dilatabilité des fluides élastiques et sur celles de la force expansive de la vapeur de l’eau et de la vapeur de l’alkool, à différentes températures. *J. Ec. Poly.*, 1:24–76, 1795.
- [9] M. Giesbrecht, G. Labahn, and W.-s. Lee. Symbolic-numeric sparse polynomial interpolation in Chebyshev basis and trigonometric interpolation. In *Proc. Workshop on Computer Algebra in Scientific Computation (CASC)*, pages 195–204, 2004.
- [10] Y. Hua and T. K. Sarkar. Matrix pencil method for estimating parameters of exponentially damped/undamped sinusoids in noise. *IEEE Trans. Acoust. Speech Signal Process.*, 38:814–824, 1990.
- [11] E. Kaltofen and W.-s. Lee. Early termination in sparse interpolation algorithms. *J. Symbolic Comput.*, 36(3-4):365–400, 2003. International Symposium on Symbolic and Algebraic Computation (IS-SAC’2002) (Lille).

- [12] H. Nyquist. Certain topics in telegraph transmission theory. *Trans. Am. Inst. Electr. Eng.*, 47(2):617–644, April 1928.
- [13] D. P. O’Leary and B. W. Rust. Variable projection for nonlinear least squares problems. *Comput. Optim. Appl.*, 54:579–593, 2013.
- [14] R. Roy and T. Kailath. ESPRIT-estimation of signal parameters via rotational invariance techniques. *IEEE Trans. Acoust. Speech Signal Process.*, 37(7):984–995, July 1989.
- [15] R. Schmidt. Multiple emitter location and signal parameter estimation. *IEEE Transactions on Antennas and Propagation*, 34(3):276–280, 1986.
- [16] C. E. Shannon. Communication in the presence of noise. *Proc. IRE*, 37:10–21, 1949.